Effect of Gold Topography and Surface Pretreatment on the Self-Assembly of Alkanethiol Monolayers

ARTICLE *in* LANGMUIR · DECEMBER 1994

Impact Factor: 4.46 · DOI: 10.1021/la00024a033

4 AUTHORS, INCLUDING:

Liang-Hong Guo
Chinese Academy of Sciences
96 PUBLICATIONS **2,440** CITATIONS

SEE PROFILE

Effect of Gold Topography and Surface Pretreatment on the Self-Assembly of Alkanethiol Monolayers

Liang-Hong Guo,[†] John S. Facci,*[,‡] George McLendon,*[,†] and Ralph Mosher[‡]

NSF Center for Photoinduced Charge Transfer, Department of Chemistry, University of Rochester, Rochester, New York 14627, and Xerox Corporation, Webster Center for Research and Technology, 114-39D, 800 Phillips Road, Webster, New York 14580

Received May 6, 1993. In Final Form: September 8, 1994[⊗]

Thin films of vapor deposited and sputtered Au are prepared as substrates for comparative studies of alkanethiol self-assembly. Vapor deposition of Au is carried out on freshly cleaved heated mica substrates in ultrahigh vacuum at 25, 150, 300, 450, and 500 °C. The Au surface roughness is controlled by the mica substrate temperature during Au evaporation becoming atomically flat at 450–500 °C as shown by AFM. Surprisingly the formation of dense blocking self-assembled alkanethiol monolayers ($CH_3(CH_2)_nSH$, n = 9, 11, 13, 15, 17) becomes greatly inhibited as the Au/mica becomes smoother. In comparison, the effect of surface pretreatment of microscopically rougher Au substrates, prepared by sputtering onto Si⟨100⟩ substrates, was also investigated. Pretreatment of Au/Si with a brief exposure to acidic peroxide combined with electrochemical potential cycling prior to alkanethiol adsorption yields pinhole-free SAMs while solvent rinse and acidic peroxide pretreatments of Au by themselves fail to do so. In contrast with previous reports, Au surface pretreatment rather than surface roughness plays the more important role in molecular self-assembly.

Introduction

Chemisorption of long-chain alkanethiols ($CH_3(CH_2)_nSH$, n = 9–20) onto Au leads to well-defined self-assembled monolayers (SAMs) whose composition and chemical and physical structure can be readily manipulated.[1-9] Because of their utility in manipulating interfacial structure at the molecular level,[10] SAMs have been used as molecular probes of diverse interfacial phenomena including ionic[11,12] and molecular[13] recognition, protein adsorption,[14] wetting,[15,16] adhesion,[17] and tribology.[18] Self-assembled redox molecule terminated alkanethiol monolayers on Au have also been used to investigate electrochemical reactions that occur over well-defined distances[19-28] controlled by the length of the methylene chain. We have investigated the properties of hybrid bilayer structures on Au[29,30] composed of an inner self-assembled monolayer and an outer electroactive Langmuir–Blodgett (L–B) monolayer.[31-38] In these bilayers the distance between the redox species, located at the monolayer–monolayer interface, and the Au electrode surface is controlled by the thickness of the SAM. During the course of preparing SAMs as inner layers for these studies, a particularly strong and unexpected influence of the Au topography and surface pretreatment on the organization and blocking characteristics of the inner monolayer was noted and is the subject of this paper.

Comparisons made by Creager and co-workers[39] of the blocking characteristics of alkanethiol monolayers adsorbed on polycrystalline Au and vapor deposited Au/Si suggested that microscopic surface roughness is a factor in alkanethiol adsorption. It was suggested that blocking monolayers were not obtained on evaporated Au/Si electrodes because of microscopic roughness on a hundred nanometer scale. Polycrystalline Au that was rendered microscopically smooth by chemical etching did, however, yield blocking SAMs. Miller et al.[27] reported the preparation of blocking self-assembled monolayers on Au/Si which

[†] University of Rochester.

[‡] Xerox Corp.

[⊗] Abstract published in *Advance ACS Abstracts,* November 1, 1994.

(1) Sagiv, J. *J. Am. Chem. Soc.* **1980**, *102*, 92.
(2) Maoz, R.; Sagiv, J. *J. Colloid Interface Sci.* **1984**, *100*, 465.
(3) Gun, J.; Iscovici, R.; Sagiv, J. *J. Colloid Interface Sci.* **1984**, *101*, 201.
(4) Bain, C. D.; Whitesides, G. M. *Angew. Chem., Int. Ed. Engl.* **1989**, *28*, 506.
(5) Whitesides, G. M.; Laibinis, P. E. *Langmuir* **1990**, *6*, 87.
(6) Strong, L.; Whitesides, G. M. *Langmuir* **1988**, *4*, 546.
(7) Bain, C. D.; Troughton, E. B.; Tao, Y.-T.; Evall, J.; Whitesides, G. M.; Nuzzo, R. G. *J. Am. Chem. Soc.* **1989**, *111*, 321.
(8) Nuzzo, R. G.; Allara, D. L. *J. Am. Chem. Soc.* **1983**, *105*, 4481.
(9) Porter, M. D.; Bright, T. B.; Allara, D. L.; Chidsey, C. E. D. *J. Am. Chem. Soc.* **1987**, *109*, 3559.
(10) Bain, C. B.; Whitesides, G. M. *Science* **1988**, *240*, 62.
(11) Rubinstein, I.; Steinberg, S.; Tor, Y.; Shanzer, A.; Sagiv, J. *Nature* **1988**, *332*, 426.
(12) Sun, L.; Johnson, B.; Wade, T.; Crooks, R. M. *J. Phys. Chem.* **1990**, *94*, 8869.
(13) Haussling, L.; Michel, B.; Ringsdorf, H.; Rohrer, H. *Angew. Chem., Int. Ed. Engl.* **1991**, *30*, 569.
(14) Prime, K. L.; Whitesides, G. M. *Science* **1991**, *252*, 1164.
(15) Bain, C. B.; Whitesides, G. M. *J. Am. Chem. Soc.* **1988**, *110*, 5897.
(16) Bain, C. B.; Whitesides, G. M. *J. Am. Chem. Soc.* **1988**, *110*, 3665.
(17) Ferguson, G. S.; Chaudhury, M. K.; Sigal, G. B.; Whitesides, G. M. *Science* **1991**, *253*, 776.
(18) Novotny, V.; Swalen, J. D.; Rabe, J. P. *Langmuir* **1989**, *5*, 485.
(19) Chidsey, C. E. D. *Science* **1991**, *251*, 919.
(20) Chidsey, C. E. D.; Bertozzi, C. R.; Putvinski, T. M.; Mujsce, A. M. *J. Am. Chem. Soc.* **1990**, *112*, 4301.
(21) Finklea, H. O.; Hanshew, D. D. *J. Am. Chem. Soc.* **1992**, *114*, 3173.
(22) Lee, K. A. B. *Langmuir* **1990**, *6*, 709.
(23) DeLong, H. C.; Buttry, D. A. *Langmuir* **1990**, *6*, 319.
(24) Uosaki, K.; Sato, Y.; Kita, H. *Langmuir* **1991**, *7*, 1510.
(25) Rowe, G. K.; Creager, S. E. *Langmuir* **1991**, *7*, 2307.
(26) Miller, C.; Cuendet, P.; Grätzel, M. *J. Phys. Chem.* **1991**, *95*, 877.
(27) Miller, C.; Grätzel, M. *J. Phys. Chem.* **1991**, *95*, 5225.
(28) Becka, A. M.; Miller, C. J. *J. Phys. Chem.* **1992**, *96*, 2657.
(29) Guo, L.-H.; Facci, J. S.; McLendon, G. L. *J. Phys. Chem.*, in press.
(30) Guo, L.-H.; Facci, J. S.; McLendon, G. L. Submitted for publication in *J. Phys. Chem.*
(31) Facci, J. S.; Falcigno, P. A.; Gold, J. M. *Langmuir* **1986**, *2*, 732.
(32) Facci, J. S. In *Molecular Design of Electrode Surfaces*; Murray, R. W., Ed.; Wiley: New York, 1992; Vol. 23; p 119.
(33) Liu, M. D.; Leidner, C. R.; Facci, J. S. *J. Phys. Chem.* **1992**, *96*, 2804.
(34) Lee, C.-W.; Bard, A. J. *J. Electroanal. Chem.* **1988**, *239*, 441.
(35) Zhang, X.; Bard, A. J. *J. Phys. Chem.* **1988**, *92*, 5566.
(36) Zhang, X.; Bard, A. J. *J. Am. Chem. Soc.* **1989**, *111*, 8098.
(37) Fujihira, M.; Aoki, K.; Inoue, S.; Takemura, H.; Muraki, H.; Aoyagui, S. *Thin Solid Films* **1985**, *132*, 221.
(38) Fujihira, M.; Araki, T. *Chem. Lett.* **1986**, 921.
(39) Creager, S. D.; Hockett, L. A.; Rowe, G. K. *Langmuir* **1992**, *8*, 854.

0743-7463/94/2410-4588$04.50/0

were then used in studies of electron transfer at these structurally defined interfaces. Self-assembled monolayers of hydroxy-terminated alkanethiol monolayers on Au/glass (similar topography to Au/Si) were also sufficiently blocking to dissolved species to study long-distance electron transfer across the polymethylene chain.[26-28] It is not clear therefore whether the differences in monolayer assembly in general can be explained by differences in surface roughness or from differences in chemical surface pretreatment.

Gold films evaporated onto heated mica substrates (300–500 °C) are microscopically smooth, containing large atomically flat terraced areas.[40] While good epitaxial growth of Au onto mica (large grain size, low surface roughness) is promoted by evaporation onto hot substrates, the best epitaxy reported requires an extended heat treatment of the mica substrate in ultrahigh vacuum prior to vapor deposition and a postdeposition annealing conducted either in air[41,42] or in vacuum.[40] Such substrates are naturally appealing for studies of the long distance electron transfer. The topography of thin film Au electrodes is controlled by the nature of the substrate, the substrate temperature, and the Au evaporation method.[39-41,43-49] The dramatic changes in Au/mica topography induced by varying the mica substrate temperature from 25 to 500 °C allow us to probe the influence of surface roughness on monolayer assembly at least for Au/mica. It is found surprisingly that alkanethiol self-assembled monolayers become significantly less blocking as the mica substrate temperature during Au evaporation is increased and, consequently, as the Au topography becomes smoother.

In contrast, Au films prepared by sputtering onto single crystal Si show a pebble-like topography and exhibit a smaller grain size than evaporated Au on Si.[41] The blocking characteristics of alkanethiol self-assembled monolayers on the much rougher sputtered Au/Si substrates are mainly dependent on the nature of the surface pretreatment, and the blocking characteristics of the latter substrates, determined by the cyclic voltammetric response of dissolved ferricyanide at the monolayer coated substrate,[9] are in all cases superior to monolayers on Au/mica. Self-assembled monolayers of alkanethiols (C_{10}–C_{18}) on Au/Si electrodes were also characterized by ellipsometry and reflection–absorption FTIR spectroscopy.

Experimental Section

Gold Film Preparation. Gold(Aldrich, 99.99 or 99.999%) was evaporated from a W filament onto freshly cleaved green muscovite mica substrates (Asheville-Schoonmaker, grade V-2). A droplet of water was applied during the separation of the mica planes to facilitate cleavage.[50] The sample stage, shown schematically in Figure 1, is fabricated in two sections from oxygen-free high-purity copper. These were clamped around a cylindrical stainless steel resistance heater in order to maintain thermal contact between the stage and heater over a wide temperature range. The entire assembly was mounted on a Macor ceramic block to minimize thermal gradient within the sample stage. This arrangement allows a stable high temperature (±3 °C at 500 °C) to be maintained with very little power, i.e. 35 W.

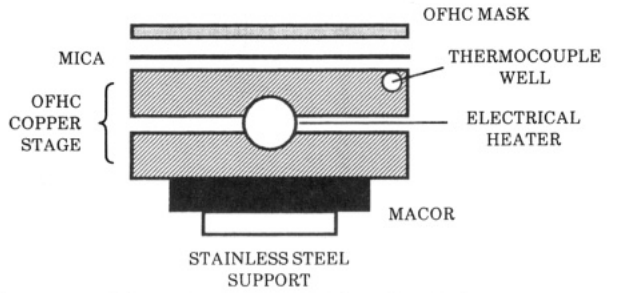

Figure 1. Schematic diagram of the ultrahigh vacuum stage for vapor deposition of Au onto heated mica substrates.

Following bakeout of the chamber, the mica substrate was prebaked at 450 °C for about 6 h[40] and then brought to the desired temperature. The pressure during Au vapor deposition was typically $1-2 \times 10^{-7}$ Torr. The Au film was annealed by further heating at the deposition temperature for 2 h. The specimen was allowed to cool at its natural cooling rate and the chamber backfilled with high-purity Ar before opening to atmosphere. Gold film thicknesses were measured by an Alpha Talystep profilometer.

Sputtered Au (200 nm) on Si substrates were obtained from Polishing Corporation of America. An interfacial layer of sputtered Ti (5 nm) was used to bond the Au layer to the wafer. The Au/Si substrates were diced with a diamond tipped stylus to a ca. 1 cm × 2 cm area and cleaned before use by one of the following procedures: (i) a simple solvent rinse, (ii) chemical etching for 10 s in hot 1:3 H_2O_2/H_2SO_4 (*CAUTION*), and (iii) a combination of (i) and (ii) followed by electrochemical potential cycling between 0 and −0.8 V vs SCE in 1.0 M KCl electrolyte (pH 6.4).

Monolayer Preparation. Solutions of 2–10 mM alkanethiols (Aldrich, TCI America) were prepared in Ar-saturated absolute ethanol shortly before each experiment. Gold electrodes were immersed in the thiol solution for 19–72 h immediately after vapor deposition (Au/mica substrates) or immediately after pretreatment (Au/Si substrates). After adsorption, the alkanethiol-coated electrodes were removed from the thiol, rinsed copiously with ethanol, and dried in a stream of high-purity Ar.

Surface Characterization. AFM and STM were done in air soon after Au deposition (Au/mica) or pretreatment (Au/Si) to image the topographic features of the Au substrates. The microscope is a commercially available Park Scientific SFM-BD2 scanning force microscope. For STM images, an electrochemically etched tungsten tip was used. The typical tunneling current and bias voltage was approximately 1 nA and 100 mV, respectively. For AFM images the surface was probed with a Si_3N_4 microfabricated cantilever with an integrated tip and a force constant of 0.032 N/m. The constant force mode of imaging was used, with an applied force of less than 5×10^{-9} N.

Conventional electrochemical apparatus was employed and all potentials are referenced to the NaCl saturated calomel electrode (SCE). Electrochemical cleaning of Au/Si substrates was performed in a conventional two-compartment electrochemical cell, while characterization of self-assembled monolayers on Au/Si and Au/mica were carried out using a noncontact cell configuration similar to the design of Koval[51] and Creager.[39] We resorted to this procedure since potential cycling of Au/mica substrates in the aqueous electrolyte frequently resulted in exfoliation of the Au film.

Ellipsometric measurements[52] were performed on monolayer films on Au/Si using an automated Rudolph Research Model ELIV ellipsometer employing 70° incident radiation (632.8 nm).

(40) DeRose, J. A.; Thundat, T.; Nagahara, L. A.; Lindsay, S. M. *Surf. Sci.* **1991**, *256*, 102.
(41) Golan, Y.; Margulis, L.; Rubinstein, I. *Surf. Sci.* **1992**, *264*, 312.
(42) Widrig, C. A.; Chung, C.; Porter, M. D. *J. Electroanal. Chem.* **1991**, *310*, 335.
(43) Chidsey, C. E. D.; Loiacano, D. N.; Sleator, T.; Nakahara, S. *Surf. Sci.* **1988**, *200*, 45.
(44) Putnam, A.; Blackford, B. L.; Jericho, M. H.; Watanabe, M. O. *Surf. Sci.* **1989**, *217*, 276.
(45) Vancea, J.; Reiss, G.; Schneider, F.; Bauer, K.; Hoffmann, H. *Surf. Sci.* **1989**, *218*, 108.
(46) Watanabe, M. O.; Kuroda, T.; Tanaka, K.; Sakai, A. *J. Vac. Sci. Technol. B* **1991**, 924.
(47) Buchholz, S.; Fuchs, H.; Rabe, J. P. *J. Vac. Sci. Technol. B* **1991**, 857.
(48) Reichelt, K.; Lutz, H. O. *J. Cryst. Growth* **1971**, *10*, 103.
(49) Emch, R.; Nogami, J.; Dovek, M. M.; Lang, C. A.; Quate, C. F. *J. Appl. Phys.* **1989**, *65*, 79.
(50) Samant, M. G.; Brown, C. A.; Gordon, G. J., II *Langmuir* **1991**, *7*, 437.
(51) Howard, J. N.; Koval, C. A. *Anal. Chem.* **1991**, *63*, 2777.
(52) Gottesfeld, S. In *Electroanalytical Chemistry*; Bard, A. J., Ed.; Marcel Dekker: New York, 1989; Vol. 15; p 143.

Superior results were obtained when freshly cleaned Au/Si electrodes were used as reference surfaces and the sample and reference surfaces had identical treatment histories. Ellipsometric constants (Δ_{film}, Ψ_{film}, Δ_{ref}, and Ψ_{ref}) were obtained on five replicate spots. Film thickness were calculated from values of $\delta\Delta = \Delta_{film} - \Delta_{ref}$ and $\delta\Psi = \Psi_{film} - \Psi_{ref}$. The ellipsometric measurements have an uncertainty of ca. 2 Å due to the uncertainty in the assumed[9] refractive index, 1.45.

Reflection–absorption infrared spectra of alkanethiolate SAMs were obtained on a Digilab Bio-Rad Model FTS65 FTIR spectrometer purged with dry N_2 and equipped with a DTGS detector. Data were accumulated by co-adding 4096 scans at a resolution of 4 cm^{-1}. Monolayer films on Au/Si substrates were examined at grazing incidence (80°) with a Spectra-Teck Model 80 fixed angle grazing incidence accessory. Reference (monolayer free) Au surfaces were cleaned by technique iii above and FTIR spectra obtained immediately after cleaning. All absorbance spectra were baseline corrected. Gold/mica substrates were not sufficiently optically flat for FTIR measurements.

Results and Discussion

Gold/Mica Substrates. X-ray diffraction of Au/mica films prepared at 25, 250, and 500 °C confirmed that the Au(111) face is parallel to the mica surface. The shifts of the (111) diffraction peaks with respect to bulk Au(111) were used to determine the strain in the Au film arising from the differential thermal coefficients of expansion of Au and mica. Gold films deposited onto 500 °C substrates exhibited a relative compressive strain of 0.17%. Slightly less strain was observed on a 300 °C specimen and no strain as expected was detected at 25 °C.

Atomic force microscope images of evaporated Au on mica substrates prepared at 150, 300, and 450 °C are shown in Figure 2. Figure 2a shows a 1.3 × 1.3 μm AFM image of Au/mica at 150 °C. The Au grain size averages 300 nm while the root-mean-square surface roughness varied from 30 to 40 Å among several samples. Figure 2b shows the expected increase in Au grain size and lowering of the surface roughness in Au/mica substrates prepared at 300 °C. The root mean square surface roughness varied from 20 to 30 Å among samples prepared at this temperature. A pronounced grain boundary and parts of several crystallites are shown in the figure. Extended areas of the Au surface are now found to be atomically flat. When Au is deposited onto 450 °C substrates, it is difficult to discern individual grains (Figure 2c). Much of the surface is characterized by large atomically flat areas. The terraces seen at the right-hand side of the figure show a variation of <3 Å over a span of 500 nm. The surface roughness of several specimens at this temperature varied from 10 to 16 Å, which is in good agreement with the value reported by Lindsay et al.[40] Notable, however, are the presence of numerous shallow 40 nm diameter depressions. The deeper depressions (10–15 Å) are associated with crystallite edges while the shallower ones (3–6 Å) are generally located within a terrace. The appearance of the pits in Figure 2c was unexpected but consistent from sample to sample. It is possible that they may result from pyrolysis of adventitious impurities which are concentrated at grain boundaries.

Alkanethiol Modified Au/Mica. Gold/mica substrates fabricated at 450, 300, and 150 °C were modified as described in the Experimental Section with alkanethiol monolayers of various chain length and subsequently electrochemically characterized in 0.1 M NaCl electrolyte containing 1.0 mM $K_3Fe(CN)_6$. Figure 3a presents the cyclic voltammetric response of ferricyanide at a Au/mica electrode (450 °C) which was exposed to a hexadecanethiol solution for 24 h. The peak-shaped cyclic voltammogram ($\Delta E_p = 420$ mV, $E^{o\prime} = 0.21$ V) indicates an array of a large number of active unblocked electrode sites resulting from

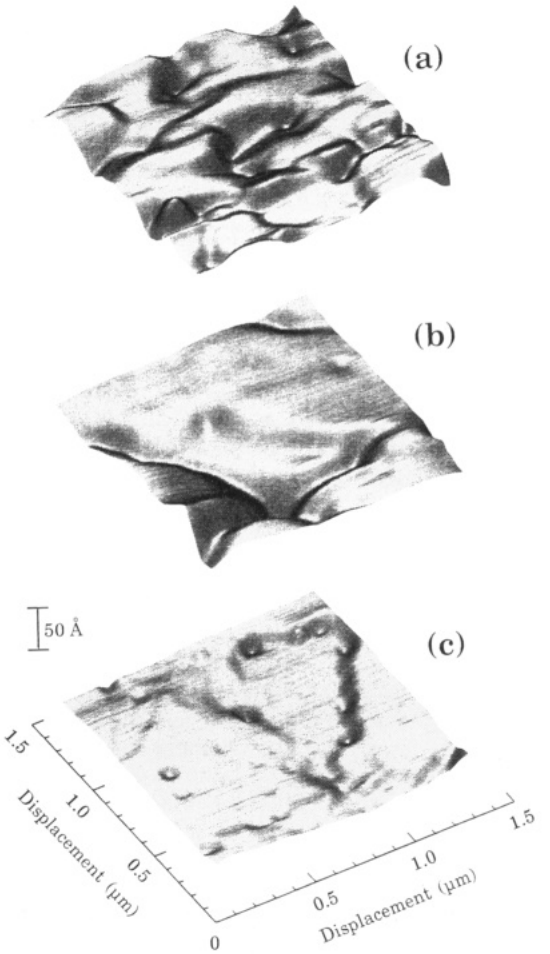

Figure 2. AFM images (1.3 × 1.3 μm) of Au films deposited on mica at (a) 150 °C, (b) 300 °C, and (c) 450 °C.

pinholes in the monolayer. Exposure to alkanethiol solutions for an additional 48 h did not substantially alter the results. In comparison the dashed curve shows the cyclic voltammogram of 1.0 mM ferricyanide at bare polycrystalline Au in 1.0 M NaCl ($E^{o\prime} = 0.18$ V, $\Delta E_p = 130$ mV). Parts b and c of Figure 3 present analogous cyclic voltammetric results for SAMs on Au/mica prepared at 300 and 150 °C, respectively. Exponential current–voltage curves are observed in the latter two cases. A completely analogous series of results were obtained on each of the 450, 300, and 150 °C Au/mica substrates when they were modified with C_{18} and C_{12} alkanethiol monolayers. Peak-shaped voltammograms were obtained on the 450 °C Au/mica substrate modified with C_{18}, C_{16}, C_{14}, and C_{12} monolayers, even for extended adsorption times. Exponentially shaped current–voltage curves were observed on the 300 and 150 °C Au/mica substrates. The dependency of the ferricyanide voltammetry on substrate temperature as opposed to chain length or adsorption time indicates that the nature of the monolayer is primarily a function of the nature of the Au surface.

The change in the voltammograms from a peaked response on high-temperature substrates to exponentially shaped on low-temperature substrates reflects a profound change in the nature of the self-assembled monolayer. Generally, three distinctly different types of voltammetric behavior are anticipated: (a) peak-shaped curves, typical of linear mass transfer arising from closely spaced defect sites in the film; (b) a sigmoidal voltammetric response characteristic of radial diffusion to isolated active sites; (c) curves that are exponentially shaped indicating kinetic currents that arise from electron transfer across a densely

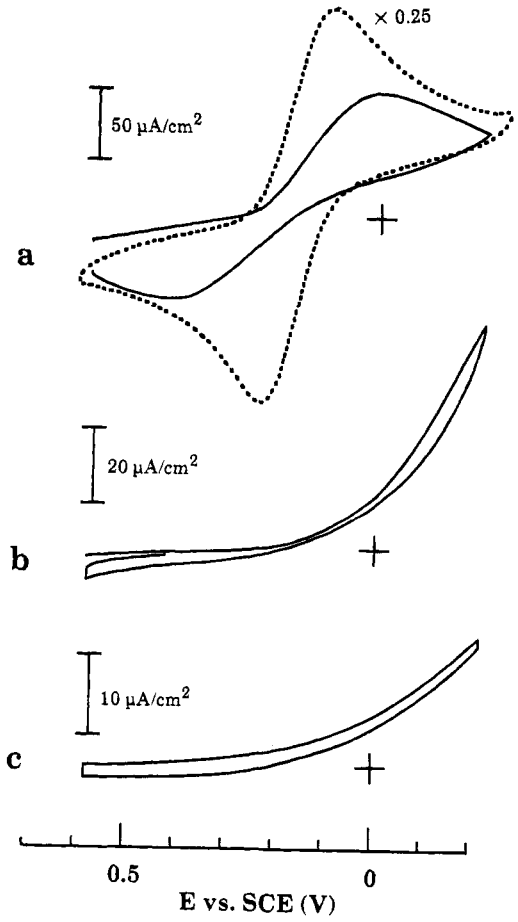

Figure 3. Cyclic voltammetric response of 1 mM $K_3Fe(CN)_6$ in 1 M NaCl at hexadecanethiol self-assembled monolayers on Au/mica electrodes prepared at (a) 450 °C (solid curve), (b) 300 °C and (c) 150 °C. The dashed curve in a is the cyclic voltammogram of 1 mM $K_3Fe(CN)_6$ in 1 M NaCl at bare polycrystalline Au. Scan rate was 100 mV/s; electrode area was 0.3 cm^2.

packed assembly of polymethylene chains. A transition among these behaviors can clearluy be seen in Figure 3.

If the self-assembled monolayer on the 450 °C substrate is characterized by a large number of closely spaced pinholes which give rise to linear diffusion of ferricyanide to the bare substrate, it is possible to estimate a minimum pinhole area by noting that the pinholes are sufficiently closely spaced such that their diffusion layers overlap. The diffusion layer of a microelectrode extends approximately $6r_0$, where r_0 is the radius of the microelectrode.[53] Therefore a lower bound of ca. 0.03 is calculated for the total area occupied by the pinholes (as opposed to the electroinactive electrode area) relative to the electrode area. Good blocking behavior exemplified by well-organized films is obtained for monolayers assembled on 150 °C substrates (Figure 3c) as well as 25 °C substrates (not shown) as indicated by the kinetic currents for reduction of ferricyanide in the figure. Intermediate behavior is obtained at 300 °C. These results are just the opposite of what would be expected if geometric considerations alone dictated the nature of the self-assembled monolayer as smoother surfaces should allow optimal packing of the molecules in a self-assembled monolayer.

It is interesting to note that pinhole defects in self-assembled alkanethiolate monolayers on vapor deposited Au/mica substrates have been observed. Haussling et al.[13] and Kim and Bard[54] reported STM images of monolayers of 11-mercaptoundecanol and octadecanethiol, respectively, assembled on Au/mica substrates (300 °C mica substrates). The STM images show a high density of nanometer sized depressions which were ascribed to defects in the monolayer rather than the underlying Au substrate. Similarly, Crooks and co-workers[12] developed the defect structure of octadecanethiol films on Au(111) single crystals by underpotential deposition of Cu within the pinholes. Edinger et al.[55] reported numerous monolayer defects (shallow 3-Å depressions) in docosanethiolate monolayer films on Au(111). It was suggested that the shallow monolayer depressions resulted from holes within the top atomic layers of the Au substrate arising from Au corrosion or surface reconstruction. Monolayer depth pinholes were not predominant. The blocking behavior of the substrates employed in the STM studies was not reported. Thus STM observations cannot be directly correlated with our electrochemical results. We attempted but were unable to obtain STM or AFM images of hexadecanethiolate monolayers on several Au/mica electrodes using previously described conditions.[55-57] Thus, at the present we postulate that the loci for pinhole formation in high-temperature substrates lies with the depressions shown in Figure 3c.

Sputtered Au on Silicon. Alkanethiol adsorption on commercially available sputtered Au/Si films which were stored in the laboratory ambient did not yield dense blocking self-assembled monolayers even at extended adsorption times (72 h). Various surface pretreatment procedures were investigated, namely solvent rinsing (pretreatment i), brief exposure to acidic peroxide (pretreatment ii), and electrochemical reduction (pretreatment iii) in order to bring the surface to a reproducibly clean state prior to alkanethiol adsorption.

Figure 4a presents a 1.3 × 1.3 μm AFM image of a clean ethanol-rinsed Au/Si. The ca. 200−nm pebble-like features of sputtered Au[41] are clearly visible. The root mean square surface roughness of the area displayed in the figure is 3.3 nm. After AFM characterization, the electrode used in Figure 4a was then briefly (10−15 s) exposed to hot H_2O_2/H_2SO_4, in order to remove any adsorbed organic material. AFM images showed essentially no difference between the latter Au substrates and the solvent-rinsed surfaces. The root mean square surface roughness of the acid peroxide treated surface is 3.4 nm. After AFM characterization, the same electrode was finally subject to several electrochemical potential cycles between 0 and −0.8 V in 1.0 M NaCl, rinsed in pure water, and dried in a stream of Ar. The AFM image of the resulting surface (Figure 4b) shows a somewhat smoother topography and a decrease in the root mean-square roughness to 2.7 nm. This small smoothing effect (ca. 20%) was reproducibly observed in several similarly treated Au/Si substrates.

Decanethiol monolayers adsorbed onto rinsed electrodes exhibited peak-shaped cyclic voltammetric waves for the reduction of ferricyanide, indicative of numerous closely spaced pinhole defects as described above. Increasing the adsorption time to 72 h did not substantially alter the results. Conversely, $C_{12}-C_{18}$ alkanethiolate modified electrodes exhibited sigmoidal voltammograms for the reduction of ferricyanide. Figure 5a illustrates for a C_{16} SAM the cyclic voltammogram for the reduction of 1 mM

(53) Wightman, R. M. *Anal. Chem.* **1981**, *53*, 1125A.

(54) Kim, Y.-T.; Bard, A. J. *Langmuir* **1992**, *8*, 1096.
(55) Edinger, K.; Gölzhäuser, A.; Demota, K.; Wöll, C.; Grunze, M. *Langmuir* **1993**, *9*, 4.
(56) Widrig, C. A.; Alves, C. A.; Porter, M. D. *J. Am. Chem. Soc.* **1991**, *113*, 2805.
(57) Alves, C. A.; Smith, E. L.; Porter, M. D. *J. Am. Chem. Soc.* **1992**, *114*, 1222.

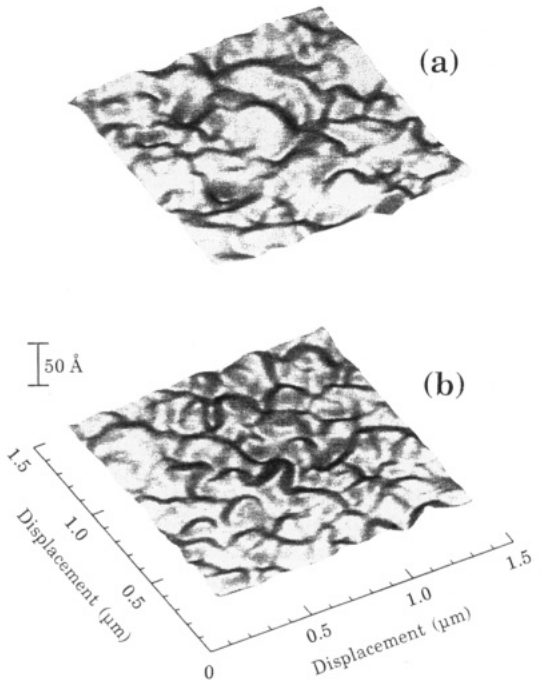

Figure 4. AFM images (1.3 × 1.3 μm) of Au/Si substrates (a) cleaned by a solvent rinse and (b) cleaned by brief immersion in acidic peroxide followed by electrochemical cycling between 0 and −0.8 V vs SCE.

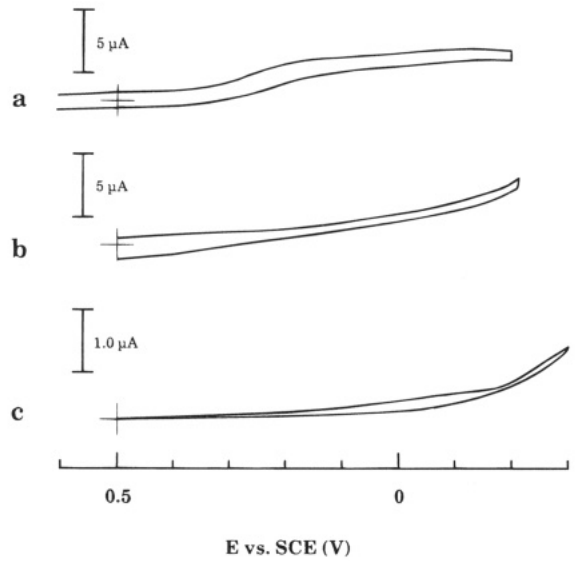

Figure 5. Cyclic voltammetric response of 1 mM $K_3Fe(CN)_6$ in 1 M NaCl at hexadecanethiol self-assembled monolayers on Au/Si electrodes after (a) solvent rinse, (b) brief immersion in hot 1:3 H_2O_2/H_2SO_4, and (c) acidic peroxide treatment plus electrochemical cycling between 0 and −0.8 V vs SCE. Scan rate was 100 mV/s. Electrode area was 0.3 cm^2.

$Fe(CN)_6^{3-}$ in 1 M NaCl. The sigmoidal shape suggests an array of isolated pinholes through which ferricyanide accesses bare Au substrate. That fewer pinholes are evidenced in the longer chain SAMs is consistent with improved coverage resulting from the greater interchain van der Waals interactions in longer chains.

Adsorption of C_{10}−C_{18} alkanethiols for 24 h on Au/Si substrates briefly immersed (10−15 s) in acidic peroxide led to monolayers which were significantly more blocking than those obtained on substrates which were rinsed in solvent. In addition, the improvement in blocking was more notable as the chain length was increased. Figure 5b illustrates for a C_{16} SAM on Au/Si treated with acid peroxide the reduction of 1 mM $Fe(CN)_6^{3-}$ in 1 M NaCl. The cyclic voltammetric response is exponentially shaped suggestive of kinetically limited current and poor permeability of dissolved ferricyanide. It would also be consistent with a reduction in the size of the pinholes to tens of nanometers.[53] The double layer capacitance (~10 μF/cm^2), measured in redox-free 1 M KCl, is higher than would be expected for a C_{16} pinhole free monolayer (~1 μF/cm^2).[9] Such high capacitance values are attributed to the ability of electrolyte ions to approach the substrate more closely than the length of an all-trans alkane chain perhaps due to thinning of the monolayer as a result of incomplete organization of film molecules.

Immersion in strongly oxidizing peroxide results in the formation of surface oxide which inhibits alkanethiol adsorption. Evidence for oxide formation was obtained from stripping cyclic voltammetric analysis of Au/Si electrodes that were exposed to acidic peroxide for 10−15 min, rinsed in high-purity water, and dried in a stream of Ar. These electrodes, which were hydrophilic, exhibited a cathodic oxide stripping peak at −0.7 V in 1 M KCl with a submonolayer coverage of $2-3 \times 10^{-11}$ mol/cm^2. Extended exposure (10−15 min) to acidic peroxide always resulted in a *higher* level of monolayer defects (pinholes) as evidenced by peak-shaped voltammograms for the reduction of ferricyanide at C_{16}-modified surfaces. Bare Au electrodes which were merely rinsed in a solvent or exposed to 1 M KCl yielded no oxide stripping peak.

Given the inhibition of alkanethiol adsorption by surface oxide, electrochemical stripping of the oxide layer should offer a pristine Au surface for self-assembly. This is in fact observed. Au/Si electrodes oxidized by exposure to acidic peroxide and subject to electrochemical potential cycling between 0 and −0.8 V exhibited the best reactivity toward alkanethiolate self-assembly as demonstrated in Figure 5c. The figure illustrates, for a C_{16} SAM on Au/Si pretreated in this manner, the cyclic voltammogram for the reduction of ferricyanide. Complete monolayer formation is implied from the excellent blocking characteristics and from the interfacial capacitance values (1−2 μF/cm^2) of several specimens. The blocking characteristics of similarly prepared C_{10}−C_{18} alkanethiolate monolayers were, in fact, always superior to those formed Au/Si cleaned by using pretreatment procedures i or ii alone. Finally, we note that the acid peroxide treatment is necessary. The use of the electrochemical potential cycling step without exposure to acidic peroxide is insufficient to yield blocking monolayers.

Pinhole densities in the latter self-assembled alkanethiol monolayer on Au have been analyzed by using a previously described procedure[9] in which the electrochemical reduction of ferricyanide is likened to reduction at an equivalent microelectrode. This analysis yields a maximum pinhole density. In the voltammogram in Figure 5c, the current at the ferricyanide $E^{\circ\prime}$ is less than 5 nA/cm^2, yielding a maximum pinhole radius of 35 μm and a maximum total pinhole area of 1×10^{-4} of the electrode area. Note that this is at least a factor of 300 less than the pinhole density in Au/mica substrates prepared at 450 °C.

Ellipsometric film thickness results for C_{10}−C_{18} SAMs on Au/Si pretreated by procedure iii are presented in Figure 6. The thickness values (filled circles) are calculated assuming bare Au substrate constants of $n_{ref} = 0.133$ and $k_{ref} = 3.61$. The expected monotonic decrease in film thickness with the diminution in carbon chain length is observed. The solid line results from an MM2 calculation of the length of an all-trans alkanethiol chain adsorbed on Au, assuming[6] a Au−S distance of 2.4 Å and a chain tilt of 30°. The data for C_{12}−C_{18} monolayers is uniformly

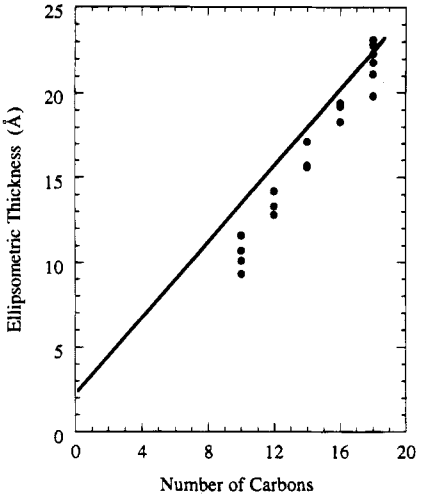

Figure 6. Ellipsometric thickness of self-assembled alkanethiolate monolayers as a function of the alkyl chain length on Au/Si electrodes subject to pretreatment iii.

displaced below that of the theoretical line while the deviation of the C_{10} data is somewhat greater due to onset of disorder. A good correspondence of the slope of the experimental data to that of the theoretical thicknesses is obtained. Physisorption of a thin film onto the reference surface is most likely responsible for the 1–2 Å offset of the average measured film thicknesses from the calculated values. Static water contact angle measurements made on C_{10}–C_{18} alkanethiolate-modified Au/Si are 106, 102, 104, 104, and 108°, respectively. These values are in good agreement with literature results and support the formation of an organized monolayer.

Grazing incidence (80°) reflection–absorption FTIR spectra of the C–H stretching region of C_{18}–C_{10} alkanethiolate monolayers on Au/Si substrates (pretreatment iii) were found to be consistent with the observation of other workers.[9] The organized nature of the monolayer can be demonstrated by the following key features: (1) the observation of the symmetric and asymmetric CH_2 stretch frequencies at 2850 and 2918 cm^{-1}, respectively, (2) the observation of the CH_3 Fermi resonance band at 2938 cm^{-1} its relative intensitivity to chain length, and (3) the low ratio of the intensities CH_2 streching vibrations to the CH_3 stretching vibration.

Self-assembled monolayers prepared by pretreatment iii were used as substrates for the deposition of Langmuir–Blodgett monolayer of 16-ferrocenylhexadecanoic acid. In these bilayer structures, ferrocene is remotely spaced from the Au substrate by the interposition of the alkanethiol monolayer. The electrochemical characterization[29] of bilayers of FCAC and self-assembled monolayers and the distance dependence of the electron transfer rates are described elsewhere.[30]

Summary and Conclusions

We have examined the influence of Au topography and surface pretreatment on the defect structure of alkanethiolate monolayers on Au. Substantially smoother Au/mica films are obtained by increasing the substrate temperature during Au evaporation. Surprisingly, the blocking characteristics of self-assembled films changes dramatically with the pinhole density increasing dramatically as the substrates become smoother. It is thought that adventitious contamination during evaporation results in Au defect sites (depressions) which are concentrated at grain boundaries. These sites may serve as the loci for pinholes in the self-assembled monolayer.

The density of molecular size defects in the alkanethiol monolayer on Au/Si is correlated to the chemical state of the surface judging from the surface pretreatment results. Substrates stored in the laboratory ambient are sufficiently fouled to prevent the formation of dense blocking monolayers. Gold/Si substrates that were pretreated with acidic peroxide exhibited a distinct improvement in the defect density even though the measured root mean square surface roughness was unchanged by this step. Extended acidic peroxide treatment actually decreases the SAM blocking ability due to the formation of a Au surface oxide. Finally, peroxide etching plus electrochemical potential cycling presents a pristine surface onto which virtually pinhole-free monolayers are assembled. Well-organized, densely packed monolayers of C_{10}–C_{18} alkanethiols were formed only when the substrates were cleaned by both the chemical etch and electrochemical reduction. Surface preparation plays at least as important a role in molecular self-assembly as surface roughness.

Acknowledgment. This work was supported in part by the National Science Foundation, (CHE-9120001). We wish to thank Dr. Howard Mizes for guidance in obtaining STM and AFM images, Dr. Shu Chang for experimental guidance in the ultrahigh vacuum work, Dr. Mary Anne Evans (Xerox) for assistance in obtaining X-ray diffraction results. L.-H. G. acknowledges useful discussions with Professor Chris Chidsey.